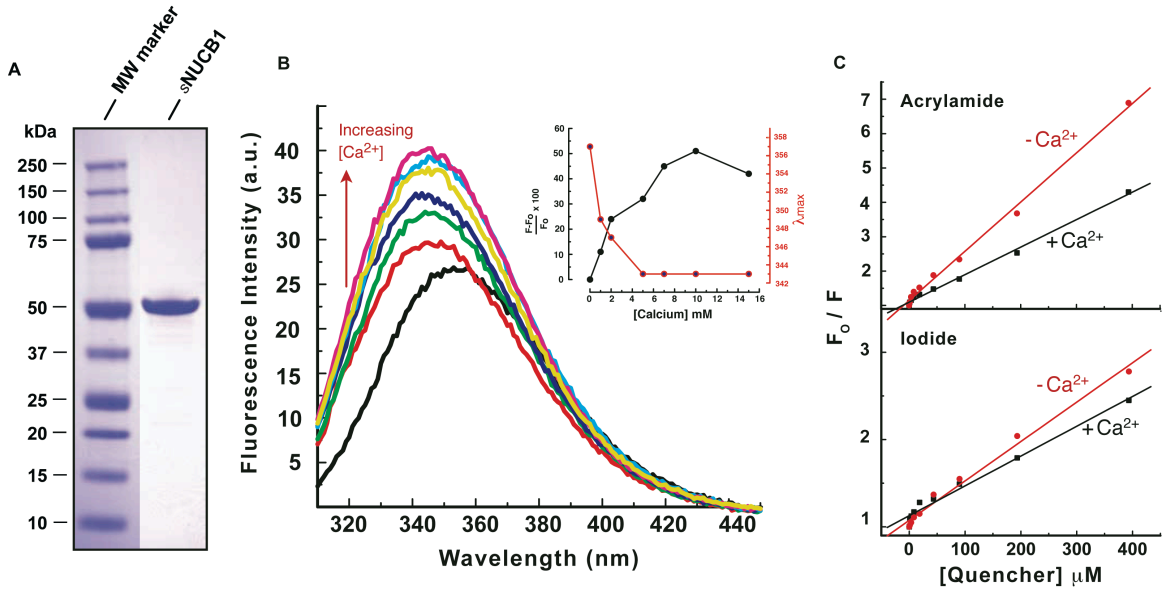
A
MW marker
sNUCB1
kDa
250
150
100
75
50
37
25
20
15
10
B
Increasing
[Ca2+]
Fluorescence Intensity (a.u.)
Wavelength (nm)
[Calcium] mM
λmax
C
Acrylamide
-Ca2+
+Ca2+
Iodide
-Ca2+
+Ca2+
Fo / F
[Quencher] μM

Fig. S1. Tryptophan residues (W233 and W333) as an intrinsic probe to monitor conformational changes associated with Ca^{2+} binding. (A) SDS-PAGE analysis of *s*NUCB1 shows a single band after final step of purification. The protein band migrates at ~ 51 kDa. (B) Ca^{2+}-free *s*NUCB1 was used for determining the conformational changes associated with Ca^{2+} binding. 178 nM *s*NUCB1 was titrated with increasing amounts of Ca^{2+} in a 3 ml cuvette while the fluorescence spectra were collected at room temperature. Fluorescence emission was collected from 310 to 460 nm with the excitation set at 295 nm. Black trace indicates Ca^{2+}-free *s*NUCB1, while the red, green, navy blue, yellow, light blue and pink traces represent 1 mM, 2 mM, 5 mM, 7 mM, 10 mM and 15 mM Ca^{2+} added to the protein. Bold arrow in red represents the increase in fluorescence intensity. Inset: Change in fluorescence intensity is indicated by black circles, while the red circles indicate the blue shift of the Trp fluorescence. With increasing concentration of Ca^{2+}, the emission intensity enhanced by 50%, while there was a 15 nm blue shift on binding to Ca^{2+} to *s*NUCB1 indicative of the movement of Trp residues from a polar environment to a non-polar, hydrophobic region. All experiments were repeated at least three times. (C) We measured the accessibility of Trp residues of *s*NUCB1 to small molecule quenchers, acrylamide and iodide, in the presence and absence of Ca^{2+}. Acrylamide is a neutral quencher while iodide is an ionic quencher and its hydrated size is larger than acrylamide. Steady-state fluorescence measurements were done in SPEX τ3 fluorimeter at 25 °C with the excitation at 295 nm, while the emission spectra were collected from 315 nm to 460 nm. Stern-Volmer plot was calculated by taking the emission maxima at 330 nm. *s*NUCB1 (333 nM with and without Ca^{2+}) in 50 mM Tris, pH 8.0, 100 mM NaCl was used and the inner filter effect was nullified by taking a very small aliquot of the quenchers from concentrated stock solutions. In the case of iodide, a small quantity of (~0.1 mM) sodium thiosulfate was added to prevent it from forming free iodide. The top panel shows the quenching of *s*NUCB1 Trp residues in the presence (black trace) and absence (red trace) of acrylamide. The bottom panel shows quenching of *s*NUCB1 Trp residues in the presence (black trace) and absence (red trace) of ionic quencher, iodide. F/F_o vs quencher concentration gave a straight line indicative of a dynamic quenching rather than static quenching. The quenching by acrylamide both in the presence and absence of Ca^{2+} was larger than the iodide showing that the two Trp residues are in different environments. Ca^{2+} binding to *s*NUCB1 caused a considerably greater decrease in the observed acrylamide quenching relative to iodide. This shows that the conformational change associated with Ca^{2+} binding reorients the Trp residues in an environment inaccessible to either quencher.

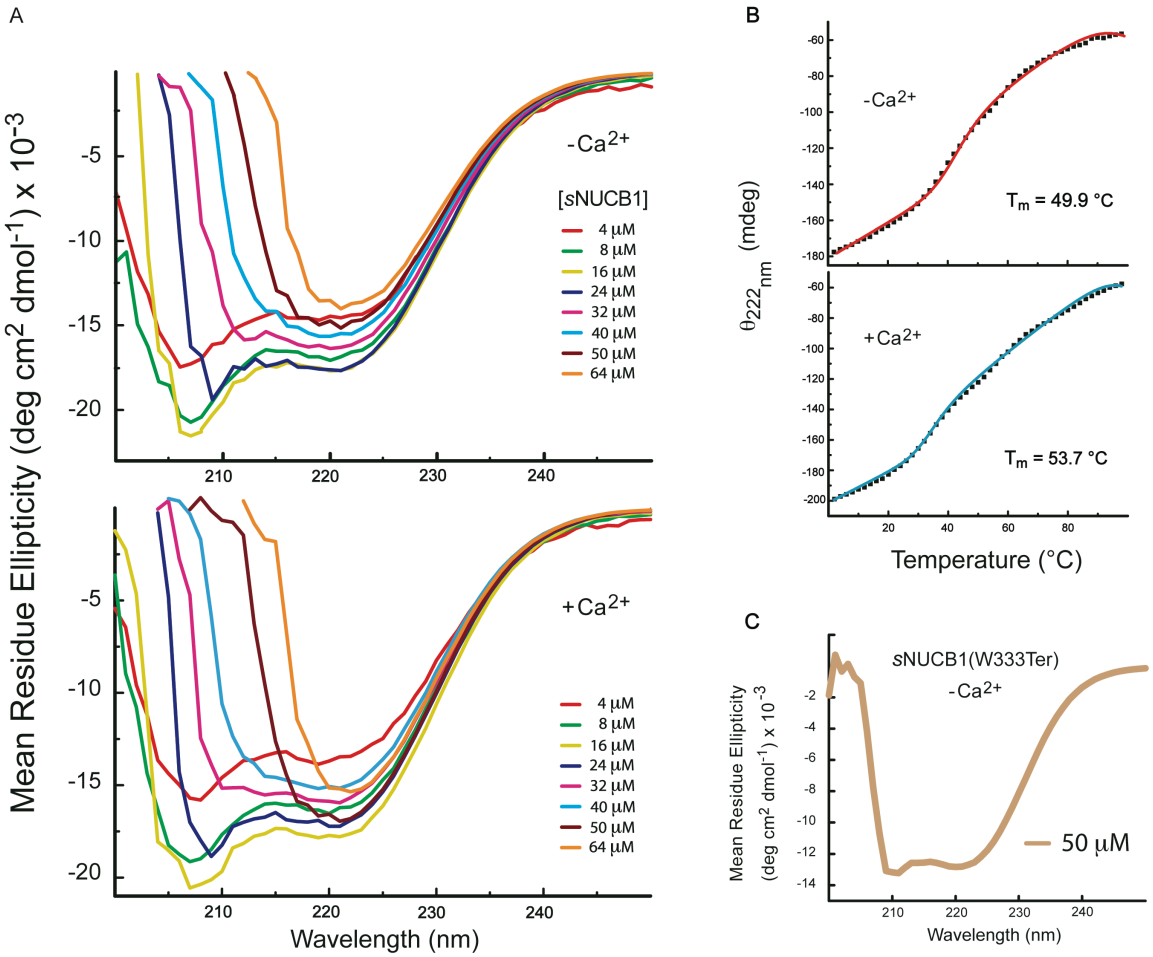
A
Mean Residue Ellipticity (deg cm2 dmol-1) x 10-3
-Ca2+
[sNUCB1]
4 µM
8 µM
16 µM
24 µM
32 µM
40 µM
50 µM
64 µM
+Ca2+
Wavelength (nm)
B
θ222nm (mdeg)
-Ca2+
Tm = 49.9 °C
+Ca2+
Tm = 53.7 °C
Temperature (°C)
C
sNUCB1(W333Ter)
-Ca2+
50 µM
Mean Residue Ellipticity (deg cm2 dmol-1) x 10-3
Wavelength (nm)

Fig. S2. Secondary structure transition in *s*NUCB1 (- / + Ca^{2+}) with increasing concentration. Far-UV circular dichroism spectra of (A) Ca^{2+}-free or (B) Ca^{2+}-bound *s*NUCB1 were collected with increasing concentration. At lower concentrations, i.e. 4 μM (red), 8 μM (green), 16 μM (yellow) and 24 μM (blue), CD spectra show that *s*NUCB1 is mainly helical. At 32 μM (pink), the CD spectrum shows a reduction in the helical content. Higher concentrations of *s*NUCB1, i.e. 40 μM (cyan), 50 μM (brown) and 64 μM (orange), show primarily β-sheet secondary structure. We also monitored thermal unfolding of *s*NUCB1. Thermal unfolding transitions of recombinant (A) Ca^{2+}-free and (B) Ca^{2+}-bound *s*NUCB1 (8 μM) were monitored by recording CD signal at 222 nm at a heating rate of $1^{o}C$ / min. The trace is indicative of a multistep non-cooperatively folded protein. The T_m for the Ca^{2+}-bound sNUCB1 is higher than T_m for the Ca^{2+}-free protein, indicating the enhanced stability of the protein in the Ca^{2+}-bound state. (C) The CD spectrum for *s*NUCB1(W333Ter) at 50 μM concentration displays a majorly helical secondary structure. In each experiment, the spectrum for buffer (50 mM Tris pH 8.0, 150 mM NaCl) alone was subtracted from each of the spectra.

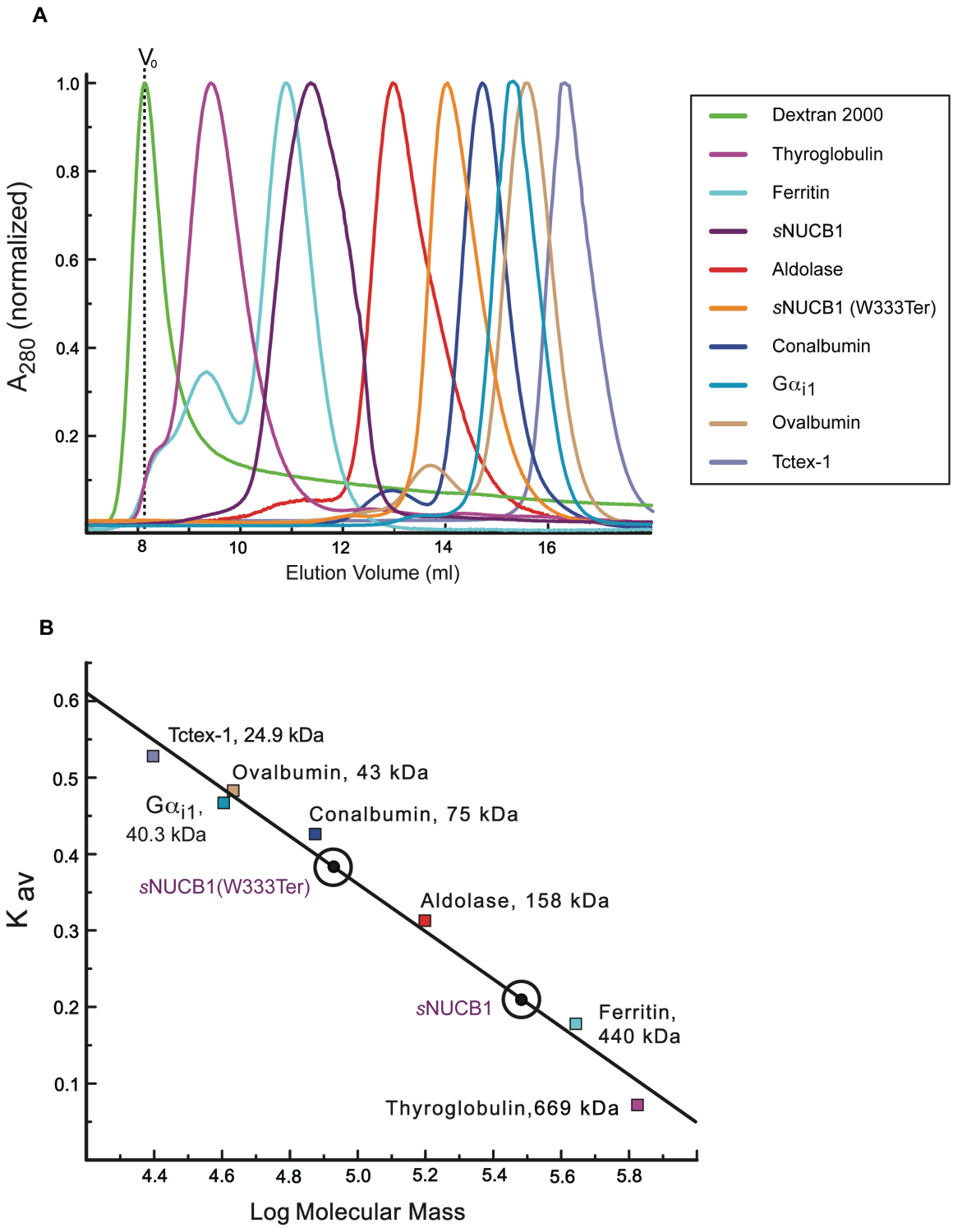
A
V0
1.0
0.8
0.6
0.4
0.2
A280 (normalized)
8
10
12
14
16
Elution Volume (ml)
Dextran 2000
Thyroglobulin
Ferritin
sNUCB1
Aldolase
sNUCB1 (W333Ter)
Conalbumin
Gαi1
Ovalbumin
Tctex-1
B
0.6
0.5
0.4
0.3
0.2
0.1
K av
Tctex-1, 24.9 kDa
Ovalbumin, 43 kDa
Gαi1,
40.3 kDa
Conalbumin, 75 kDa
sNUCB1(W333Ter)
Aldolase, 158 kDa
sNUCB1
Ferritin,
440 kDa
Thyroglobulin,669 kDa
4.4
4.6
4.8
5.0
5.2
5.4
5.6
5.8
Log Molecular Mass

Fig. S3. Size-exclusion chromatography (SEC) of *s*NUCB1 and molecular weight standards. (A) SEC of *s*NUCB1, heavy molecular weight standards (GE Health Sciences) along with known globular proteins was done using a Superdex200 10/30 HR column. Proteins were individually injected onto the column and the absorbance normalized elution profile for each protein was plotted as a function of elution volume. (B) The void volume (V_o) of the column is derived from the elution of Blue Dextran, whereas elution volume (V_e) for each protein is obtained from the corresponding peak for each sample. In order to estimate the molecular mass of *s*NUCB1 and *s*NUCB1(W333Ter), a calibration curve was prepared by plotting K_{av} $[(V_e-V_o)/(V_c-V_o)]$ vs log(molecular weight) where V_c is the geometric volume of the column. The data were fit to a linear equation. The estimated molecular mass of *s*NUCB1 and *s*NUCB1(W333Ter) were obtained from the plot by using their corresponding K_{av} values.

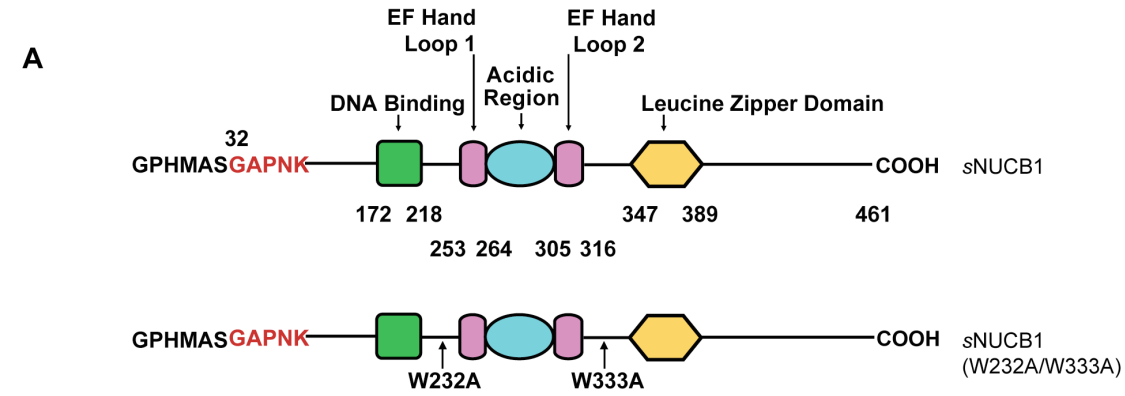
A
EF Hand Loop 1
EF Hand Loop 2
Acidic Region
DNA Binding
Leucine Zipper Domain
32
GPHMASGAPNK
COOH
sNUCB1
172 218
253 264
305 316
347 389
461
GPHMASGAPNK
COOH
sNUCB1 (W232A/W333A)
W232A
W333A

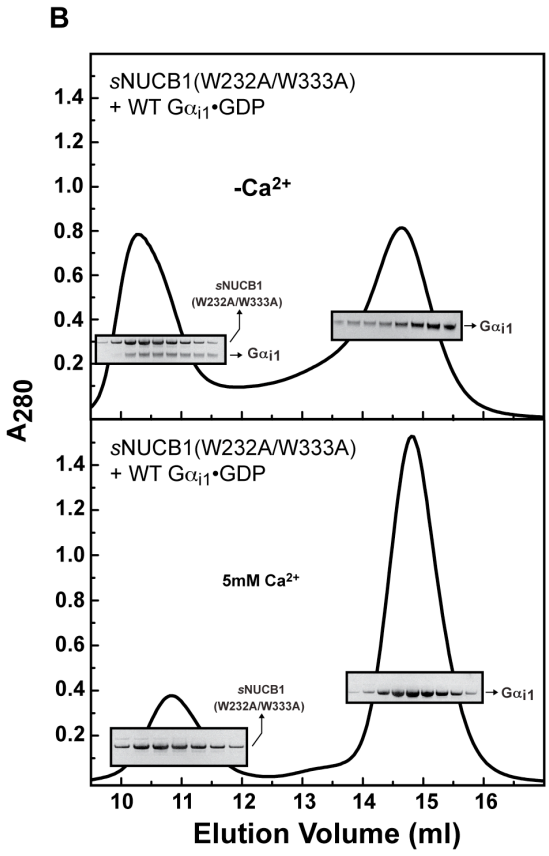
B
sNUCB1(W232A/W333A) + WT Gαi1•GDP
-Ca2+
sNUCB1 (W232A/W333A)
Gαi1
5mM Ca2+
A280
Elution Volume (ml)

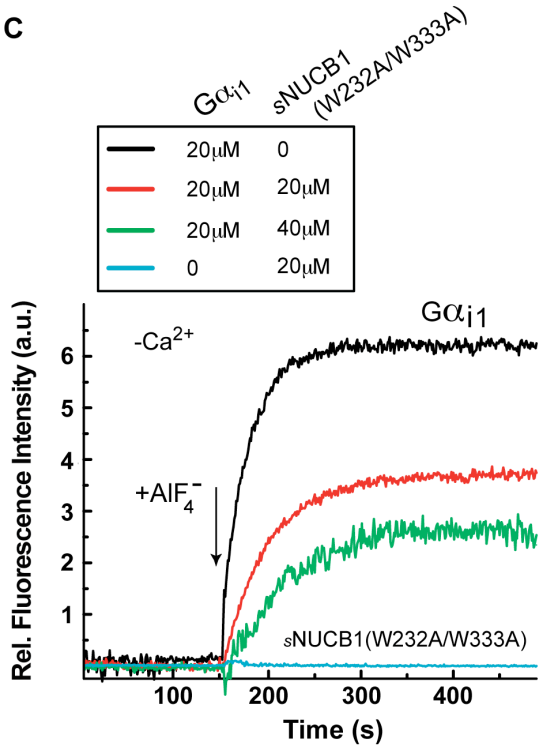
C
Gαi1
sNUCB1 (W232A/W333A)
20μM 0
20μM 20μM
20μM 40μM
0 20μM
-Ca2+
+AlF4-
sNUCB1(W232A/W333A)
Rel. Fluorescence Intensity (a.u.)
Time (s)

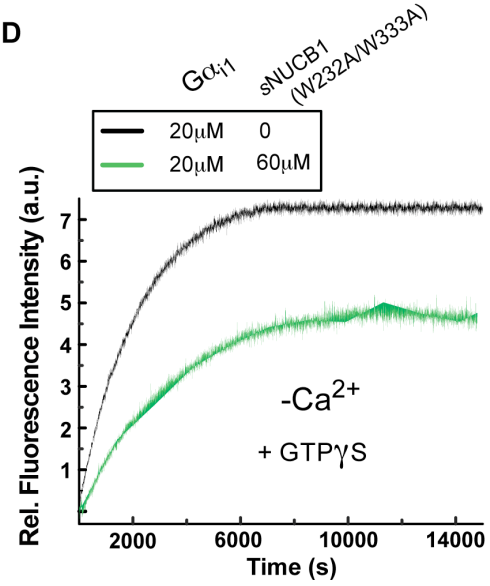
D
Gαi1
sNUCB1 (W232A/W333A)
20μM 0
20μM 60μM
-Ca2+
+ GTPγS
Rel. Fluorescence Intensity (a.u.)
Time (s)

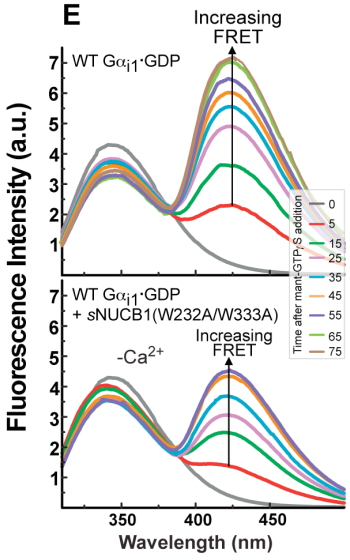
E
Increasing FRET
WT Gαi1•GDP
WT Gαi1•GDP + sNUCB1(W232A/W333A)
-Ca2+
Time after mant-GTPγS addition
Fluorescence Intensity (a.u.)
Wavelength (nm)

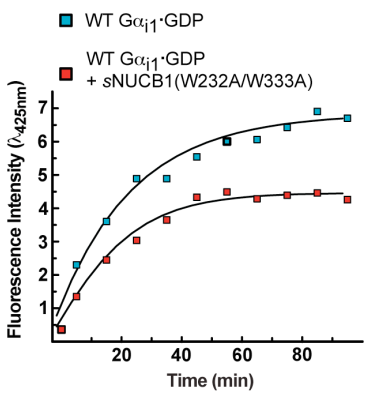
WT Gαi1•GDP
WT Gαi1•GDP + sNUCB1(W232A/W333A)
Fluorescence Intensity (λ425nm)
Time (min)

Fig. S4. *s*NUCB1 affects nucleotide-exchange by WT $G\alpha_{i1}$. (A) The domain diagram of *s*NUCB1 highlights the modular structure of protein. Trp residues in the sequence of *s*NUCB1 that were mutated to generate *s*NUCB1(W232A/W333A) are listed below it. (B) We first used size-exclusion chromatography to establish the nature of interaction between *s*NUCB1(W232A/W333A) and $G\alpha_{i1}$ in solution under several conditions. *s*NUCB1(W232A/W333A) and $G\alpha_{i1}$•GDP were incubated together in the absence (*upper*) or presence (*lower*) of Ca^{2+} and the mixture was subjected to size-exclusion chromatography using a Superdex200 10/30 HR column. Peak fractions were analyzed by SDS-PAGE with Coomassie-brilliant blue staining as shown in the insets. As shown, *s*NUCB1(W232A/W333A) and $G\alpha_{i1}$•GDP form a complex only in the absence of Ca^{2+} and not when Ca^{2+} is bound to *s*NUCB1(W232A/W333A). Further, to investigate the effect of *s*NUCB1 / *s*NUCB1(W232A/W333A) on nucleotide exchange (C) we employed a time-based intrinsic Trp fluorescence assay to measure the rate of spontaneous nucleotide exchange by $G\alpha_{i1}$•GDP in the presence of increasing concentrations of *s*NUCB1. The fluorescence emission of Trp211, which is situated on the Switch II region of $G\alpha_{i1}$ increases dramatically on binding of AlF_4^- to $G\alpha_{i1}$•GDP. To eliminate the influence of intrinsic Trp fluorescence from *s*NUCB1 on the measured activation rates, we used site-directed mutagenesis to engineer a Trp free version of *s*NUCB1, *s*NUCB1(W2323A/W333A). $G\alpha_{i1}$•GDP alone (20 μM, black trace) was allowed to equilibrate while Trp fluorescence emission was recorded at 340 nm. Thereafter, AlF_4^- (20 mM) was injected at 180 seconds and the fluorescence time course was monitored. The same experiment was repeated in the presence of increasing concentrations of *s*NUCB1(W232A/W333A). The rate of $G\alpha_{i1}$•GDP activation by AlF_4^- is considerably decreased upon preincubation with equimolar (red) or excess (green) *s*NUCB1(W2323A/W333A). As a control, *s*NUCB1(W232A/W333A) alone shows no enhancement in Trp fluorescence upon addition of AlF_4^- (blue). (D) In an analogous experiment, we monitored the enhancement in fluorescence emission of Trp211 upon exchange of GDP for GTPγS, a non-hydrolyzable analogue of GTP. The results show that the rate and extent of GTPγS-mediated activation is less when $G\alpha_{i1}$•GDP is bound to Ca^{2+}-free *s*NUCB1(W232A/W333A). (E) $G\alpha_{i1}$•GDP activation was also monitored through exchange of bound GDP for fluorescent mant-GTPγS nucleotide. Upon uptake of mant-GTPγS by $G\alpha_{i1}$, Trp211 moves into the catalytic pocket and forms a productive FRET pair which can transfer energy to the nucleotide analogue mant-GTPγS. FRET from Trp211 of $G\alpha_{i1}$ to bound mant-GTPγS was measured at different times after addition of mant-GTPγS. The same experiment was carried out in the presence of *s*NUCB1(W2323A/W333A). The addition of *s*NUCB1(W2323A/W333A) caused a decrease in the rate of FRET increase, indicating that uptake of mant-GTPγS by $G\alpha_{i1}$ was inhibited. Maximum FRET intensity at 425 nm with increasing time was plotted. A fit to each data set clearly shows attenuation of FRET intensity for $G\alpha_{i1}$ complexed to Ca^{2+}-free *s*NUCB1(W232A/W333A) in comparison to $G\alpha_{i1}$ alone, suggesting that Ca^{2+}-free *s*NUCB1(W232A/W333A) inhibits nucleotide exchange.

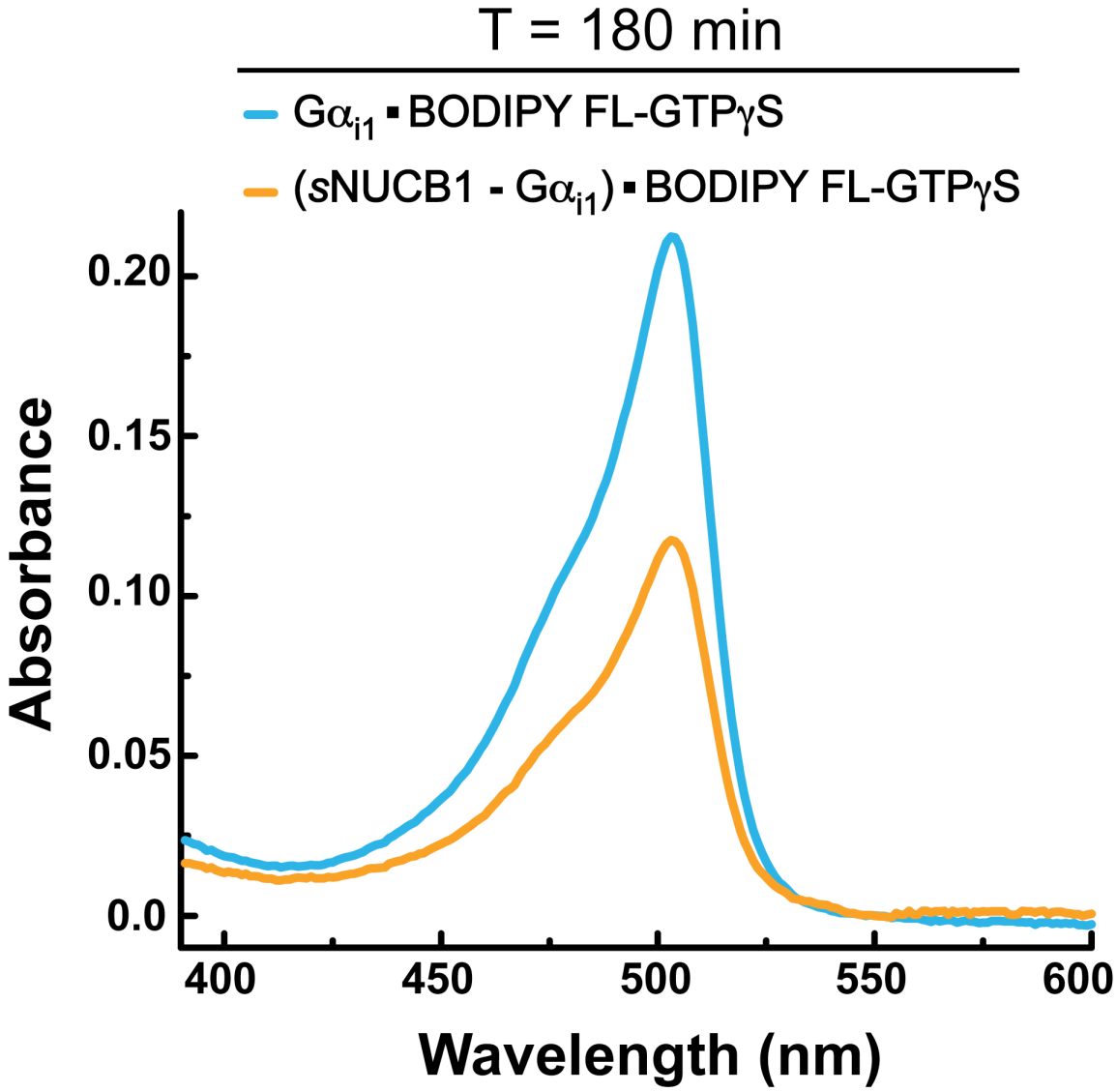
T = 180 min
Gαi1 ▪ BODIPY FL-GTPγS
(sNUCB1 - Gαi1) ▪ BODIPY FL-GTPγS
Absorbance
0.20
0.15
0.10
0.05
0.0
400
450
500
550
600
Wavelength (nm)

Fig. S5. BODIPY FL-GTPγS absorbance. The absorbtion spectrum for BODIPY FL-GTPγS bound to WT $G\alpha_{i1}$ alone (20 μM) (blue) or in complex with Ca^{2+}-free *s*NUCB1 (100 μM) (orange) after 180 min is shown. The wavelength scans show that absorbance maxima for BODIPY fluorophore does not change on binding of Ca^{2+}-free *s*NUCB1 to $G\alpha_{i1}$.

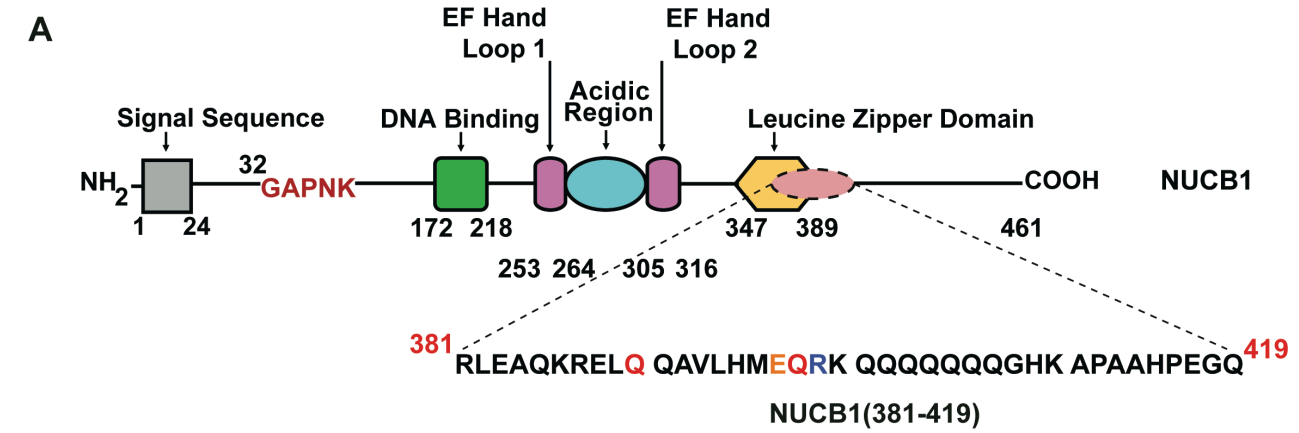

B

rAGS3_GL1	DEECFFDLLSKFQSSRMDDQRCPLEEGQAGAAEATA---
rAGS3_GL2	QTEEFFDLIASSQSRRLDDQRASVGSLPGLR-ITLNN--
rAGS3_GL3	GDE-FFNMLIKYQSSRIDDRQCPPPDVLPRGPTMPD---
rAGS3_GL4	D-EDFFSLIQRVQAKRMDEQRVDLAGSPDQEAS--GLP-
hGPSM2_GL1	GDEGFFDLLSRFQSNRMDDQRCCLQEKNCHTASTTTSST
hGPSM2_GL2	NTDEFLDLLASSQSRRLDDQRASFSNLPGLR-LTQNSQS
hGPSM2_GL3	ADEDFFDILVKCQGSRLDDQRCAPPPATTKGPTVPDED-
hGPSM2_GL4	D-EDFFSLILRSQGKRMDEQRVLLQRDQNRDTDF-GLKD
mPCP-2_GL1	DQEGFFNLLTHVQCDRMEEQRCSLQAGPGQNPESQG-
mPCP-2_GL2	EMDNLMDMLVNTQGRRMDDQRVTVNSLPGFQPIGPKD--
RGS12_GL1	EAEEFFELISKAQSNRADDQRGLLRKEDLVLPEFLR---
RGS14_GL1	DIEGLVELLNRVQSSGAHDQRGLLRKEDLVLPRFLQ---
hNUCB1 (381-419)	RLEAQKRELQ--QAVLHMEQRKQQQQQQQGHKAPAAHP-

* ***

C

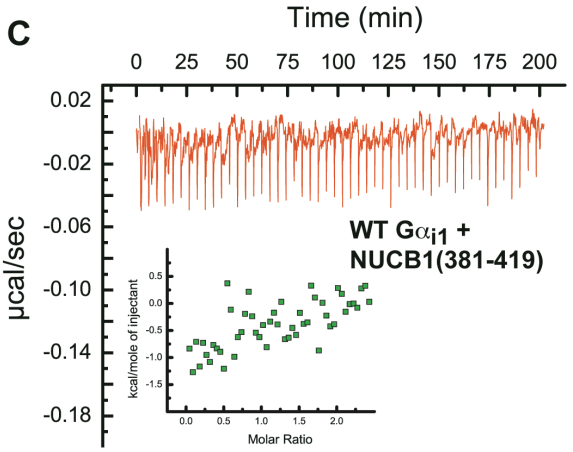

Fig. S6. NUCB1(381-419) does not bind to WT $G\alpha_{i1}$•GDP. (A) A CT 39 mer sequence of NUCB1 (residues 381-419) consist of the Glu-Gln-Arg (397-399) triad preceded by an upstream Gln390. (B) The sequence alignment of NUCB1(381-419) with various GoLoco motif peptides shows the presence of the conserved Gln and the Asp/Glu-Gln-Arg motif in the sequence. The stars indicate the positions of the conserved residues amongst different sequences. (C) We further used ITC to measure the binding of NUCB1(381-419) to WT $G\alpha_{i1}$•GDP. NUCB1(381-419) (600 μM) was injected into a buffered solution of WT $G\alpha_{i1}$•GDP (40 μM) in the reaction cell and the heat released per injection was recorded. The heat of dilution for the addition of $G\alpha_{i1}$•GDP to buffer alone was subtracted. The isotherm shows complete absence of any binding event indicating that NUCB1(381-419) does not interact with WT $G\alpha_{i1}$•GDP.

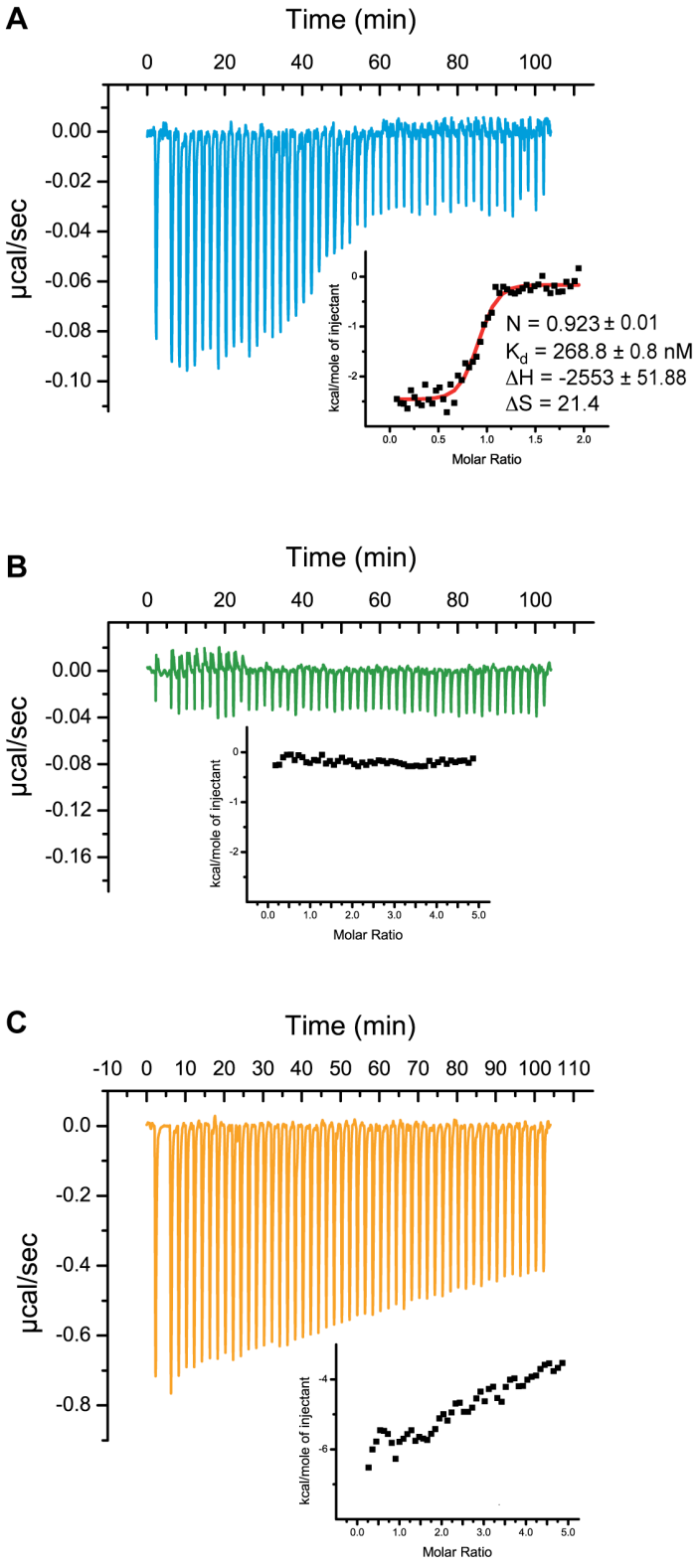
A
Time (min)
0
20
40
60
80
100
0.00
-0.02
-0.04
-0.06
-0.08
-0.10
µcal/sec
kcal/mole of injectant
0
-1
-2
0.0
0.5
1.0
1.5
2.0
Molar Ratio
N = 0.923 ± 0.01
K_d = 268.8 ± 0.8 nM
ΔH = -2553 ± 51.88
ΔS = 21.4
B
Time (min)
0
20
40
60
80
100
0.00
-0.04
-0.08
-0.12
-0.16
µcal/sec
kcal/mole of injectant
0
-1
-2
0.0
1.0
2.0
3.0
4.0
5.0
Molar Ratio
C
Time (min)
-10
0
10
20
30
40
50
60
70
80
90
100
110
0.0
-0.2
-0.4
-0.6
-0.8
µcal/sec
kcal/mole of injectant
-4
-6
0.0
1.0
2.0
3.0
4.0
5.0
Molar Ratio

Fig. S7. *s*NUCB1 inhibits binding of RGS14(496-531) to $G\alpha_{i1}$•GDP. **(A)** We perfomed ITC experiments to measure binding to RGS14(496-531) peptide to $G\alpha_{i1}$•GDP. The heat released per injection of aliquots of a solution of RGS14(496-531) (200 μM) into a buffered solution of $G\alpha_{i1}$•GDP (20 μM) was recorded and the area under the curve was integrated. The heat of dilution for the addition of RGS14(496-531) to buffer alone was subtracted. A non-linear least squares fit of the calculated values using the "one-set of sites" model for WT $G\alpha_{i1}$•GDP resulted in a satisfactory fit with a dissociation constant of 268 ± 0.01 nM as shown in the *inset*. Thereafter we performed ITC experiments to measure binding of RGS14(496-531) (500 μM) to 20 μM buffered solution of $G\alpha_{i1}$•GDP precomplexed to Ca^{2+}-free **(B)** *s*NUCB1 or **(C)** *s*NUCB1(W333Ter). The corresponding *insets* show lack of any substantial heat release due to complete absence of binding. Thus, binding of either *s*NUCB1 or *s*NUCB1(W333Ter) completely inhibits RGS14(496-531) binding to $G\alpha_{i1}$•GDP.